COE-Based Low-Reflectivity Integrated-Black and High-Brightness Wide-Color-Gamut Display Technology

Ying Shen*, Xiaojing Liu*, Hongyu Wang*, Yu Gao*, Chenzhe Li*, Mihwa Ha*, Wonjun Song*, Xiujian Zhu*

*** Hefei Govisionox Technology Co., Ltd. (Visionox's Affiliated Company) Anhui, P. R. China**

Abstract

Building on Visionox's award-winning COE flexible AMOLED at SID 2025, this work optimizes reflectance, reflection hue, color gamut, and luminance by spectrally matching CFs and OLED emission, with a transition layer and AR film, achieving industry-leading <1% reflectance and better integrated-black, while a tandem device with UBA delivers >4000 nits luminance, ~98.65% BT.2020 coverage, and ~20–40% lower panel power than the previous generation.

Author Keywords

Color filter on encapsulation; High brightness; Wide color gamut; Low reflectivity; Integrated-black.

1. Introduction

OLED displays employing external polarizers suffer from severe optical losses and increased module thickness, which are unfavorable for emerging form-factor terminals such as foldable smartphones. Consequently, the OLED displays of current flagship foldable devices primarily adopt polarizer-free OLED technology, also known as COE (Color Filter on Encapsulation). In COE, the conventional circular polarizer is replaced by color filters (CFs) and a black matrix (BM), which together suppress reflections and mitigate color crosstalk, thereby preserving color purity and contrast, as illustrated in **Figure 1a**. Compared with traditional polarizer-based (POL) solutions, COE technology offers distinct advantages in luminance, power consumption, color gamut, and module thickness, as shown in **Figure 1b**.Visionox's low-reflectivity COE flexible AMOLED technology demonstrator (**Figure 1c**) was selected by professional attendees for the *Best New Display Component award* in the *People's Choice Awards* at *SID Display Week 2025*. This COE panel exhibits a reflectance as low as 1.3%, which enhances visual clarity, reduces disturbance from strong ambient light, and delivers more natural color reproduction. Relative to conventional POL solutions, it reduces power consumption by more than 20% and thins the overall module by about 100 μm, enabling lighter and more efficient displays. This achievement has set a benchmark and played a leading role in the development of low-reflectivity COE technology.

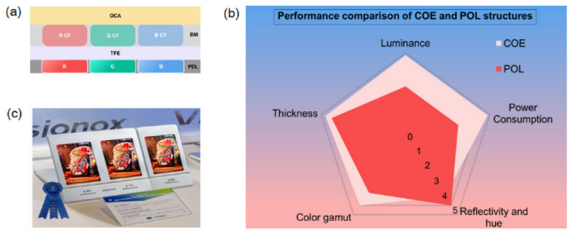

Figure 1. Visionox's low-reflectivity COE demonstrator first unveiled globally in 2025. (a) Schematic of the COE structure. (b) Performance comparison between COE and POL products. (c) Photograph of the award-winning low-reflectivity COE demonstrator at SID 2025.

With the continuous enhancement of image-quality requirements in mobile devices, automotive displays, and extended-reality systems, low reflectance with an integrated-black off state, together with high-brightness wide-color-gamut display, has become a core competitive metric for next-generation OLED technologies. However, commercially mass-produced COE products still have room for improvement in terms of extreme low reflectance, reflection hue, BT.2020 color-gamut coverage, and full-screen luminance. These are key technical challenges that panel makers commonly face and urgently need to overcome in mass-production products, and they are also among the crucial metrics Visionox must address to usher in the AMOLED+ era.

To tackle these issues, this work proposes optimization strategies for extreme reflectance reduction and integrated-black appearance based on the COE architecture. By reducing the pixel aperture ratio, developing CF materials spectrally matched to narrow-band pTSF emission, and introducing a refractive-index transition layer above the CF to mitigate refractive-index discontinuities, the panel reflectance can be reduced below 1%, reaching an industry-leading ultra-low-reflectance level. To further enhance the integrated-black appearance, we optimize CF thicknesses in simulation and design an AR coating with a tailored reflection spectrum, achieving a lower reflectance than comparable POL products under similar conditions, while maintaining lower power consumption. Moreover, tandem device structures and the UBA are incorporated into this stack. Simulation results predict a full-screen luminance exceeding 4000 nits, with a 20%–40% power-consumption improvement relative to previous-generation COE panels. The overlap with the BT.2020 color gamut reaches approximately 98.65%. Thus, this work attains industry-leading performance in reflectance, reflection hue, luminance, and color gamut.

2. Results and Discussion

2.1. Low-reflectivity integrated-black optimization

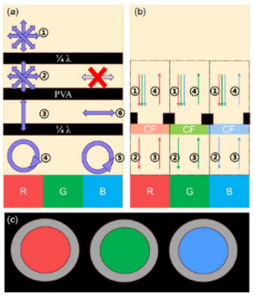

Figure 2. Schematic comparison of circular-polarizer and COE panel structures. (a) Circular-polarizer structure; arrows indicate the polarization state and propagation path of ambient light. (b) COE panel structure; arrows indicate the incident paths of ambient light at different wavelengths. (c) Top view of a simplified COE layout.

Figures 2a and **2b** compare the panel structures of POL-based and COE products. In the POL architecture, most incident ambient light is absorbed after passing through the polarizer and λ/4 plate, providing strong suppression of ambient reflections. In the COE structure, by contrast, the circular polarizer is replaced by CF and BM layers. Reflection suppression relies on spectral filtering by the CF and spatial blocking by the BM. As a result, more ambient light is reflected toward the viewer compared with POL solutions, making viewing under strong ambient conditions relatively more challenging.

Figure 2c shows a simplified top view of the COE layout, which consists of the pixel aperture area, the pixel-define layer area (PDL), and the BM opening area. The total panel reflectance can be approximated as the weighted sum of the reflectance contributions from the pixel-aperture and non-aperture regions,

$$R_{Panel} = R_{Pixel} \times A_{Pixel} + R_{non\text{-}pixel} \times A_{non\text{-}pixel} \quad (1)$$

where (R) denotes the reflectance of each region and (A) is the corresponding area fraction [1]. Owing to metallic electrodes and other components, the reflectance of the pixel aperture region is typically higher than that of non-aperture regions. Therefore, reducing the reflectance in the pixel aperture region and/or decreasing its area fraction are both effective pathways to lower total panel reflectance.More specifically, reducing the pixel aperture ratio (A_{Piexl})) can lower reflectance, but an excessively small aperture may degrade luminance lifetime and lead to a grainy display appearance. Increasing CF thickness can reduce pixel reflectance (R_{Pixel}), but at the cost of optical efficiency. Because overall reflectance is the weighted average over the visible-spectrum reflectance, narrowing the CF transmission band can also reduce (R_{Pixel}), yet again with an efficiency penalty. These straightforward approaches therefore tend to trade improved reflectance against lower efficiency or degraded uniformity. Fortunately, by combining these structural optimizations with our narrow-band OLED emission technology, we can narrow the CF transmission window while suppressing reflectance without sacrificing efficiency.

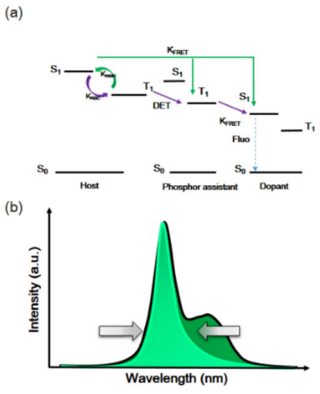

Figure 3. Energy-transfer mechanism and narrow-spectrum characteristics of the pTSF emission system. (a) Schematic of the energy-transfer process in pTSF materials. (b) Illustration of OLED emission-spectrum narrowing; the FWHM of pTSF green emission can be compressed to several tens of nanometers.

Our in-house pTSF materials exhibit significantly narrower emission spectra [2–5]. These materials adopt a multi-sensitization strategy to achieve narrow-band emission. As illustrated in **Figure 3**, the pTSF energy-transfer mechanism enables a photoluminescence full width at half maximum (FWHM) of only several tens of nanometers for the green emission, which is much narrower than that of typical Ir-based green emitters. Narrower emission spectra not only compensate the brightness loss associated with narrowed CF transmission windows but also enhance color purity and effectively broaden the achievable color gamut.

CF Material Design. The narrow emission of pTSF devices allows the CF transmission band to be narrowed by a similar extent without compromising the transmitted luminance of the pTSF devices, thereby maintaining high efficiency in COE. A new CF material with a narrow transmission band specifically optimized for pTSF has therefore been developed.

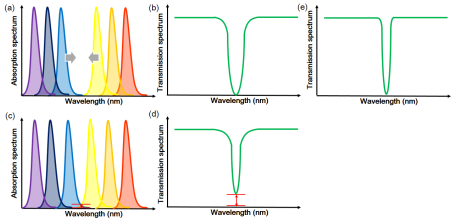

Figure 4. Schematic of CF chromophore absorption and transmission spectra. (a) and (c) Examples of different superpositions of chromophore absorption peaks. (b) and (d) Schematic transmission bandwidth and intensity corresponding to the absorption configurations in (a) and (c). (e) Ideal CF absorption spectral shape.

In COE structures, the CF materials are typically fabricated using pigment-dispersion techniques. The CF is essentially a photosensitive resin material in which the spectral characteristics are realized by designing appropriate chromophores to obtain a target absorption spectrum.

The CF transmission spectrum is the combined result of all pigments, resins, and overcoat (OC) layers, and its optical density can be described by the Beer–Lambert law [6],

$$A(\lambda) = -log_{10}\left(\frac{P}{P_0}\right) = abc \quad (2)$$

where A(λ) is the absorbance at wavelength (λ), P is the transmitted radiant powers, a is the absorptivity, b is the effective optical path length in the absorbing medium, and c is the concentration of the absorbing species. Because multiple pigments coexist in the CF, their absorption spectra superpose, resulting in a finite transmission window within a specific wavelength range, while most of the remaining wavelengths are strongly absorbed, as shown in **Figures 4a** and **4b**.

During CF transmission-spectrum development, our design target is to obtain high transmission within the passband and steep cutoffs outside the passband, as illustrated in **Figure 4e**. Although shifting chromophore peak positions can narrow the transmission FWHM, the tail-overlap of the absorption peaks can reduce the transmission at the desired passband center, leading to efficiency loss, as depicted in **Figures 4c** and **4d**. The key challenge therefore lies in suppressing the tail absorption of the chromophore peaks. By extending π-conjugation, introducing appropriate auxochromes/hyperchromic groups, and tuning donor–acceptor strength through molecular design, the absorption peaks can be precisely positioned within the target color range, enabling selective absorption while minimizing FWHM and reducing “tail” absorption into adjacent wavelength ranges. The

CF materials developed in this work exhibit high absorption in the stopband, high transmission in the passband, and a narrow, steep transmission window, which approximates the ideal spectral shape.

Refractive-index transition-layer design. In addition to the CF transmission spectrum itself, Fresnel reflection at interfaces also contributes non-negligibly to the panel reflectance in COE structures. The refractive-index difference between the CF and the overlying medium induces additional reflection at the interface. To mitigate this effect, a refractive-index transition layer is introduced between the CF and the upper dielectric. By appropriately setting the thickness and refractive index of this transition layer, the refractive-index discontinuity between adjacent films is reduced, thereby lowering interface reflection. Under the same ambient-light conditions, the required panel luminance can thus be further reduced while achieving purer colors.

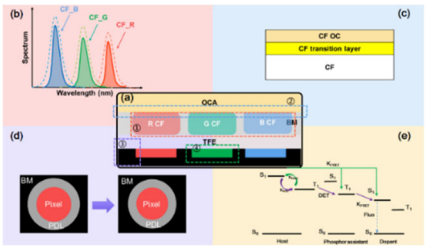

Figure 5. Integrated optimization scheme for extreme low reflectance. The dashed box highlights the optimized components. (a) COE stack structure. (b) CF transmission-spectrum optimization. (c) Refractive-index transition-layer optimization. (d) Pixel-aperture optimization. (e) Narrow-emission-spectrum optimization.

Based on the above considerations, we propose a combined optimization strategy: moderately reduce the pixel aperture ratio while preserving display quality, narrow the CF transmission spectrum, and introduce a refractive-index transition layer above the CF. As illustrated in **Figure 5**, this scheme effectively reduces reflection from the pixel-aperture region and mitigates additional reflection induced by refractive-index jumps at interfaces. Simulation results show that the pixel aperture ratio cannot be arbitrarily reduced without degrading display quality; hence, reflectance reduction by aperture scaling alone is limited. With the proposed COE architecture combined with a conventional AR coating, an ultra-low reflectance can already be achieved. Compared with the 1.33% reflectance of our award-winning COE demonstrator in 2025, the new COE-oriented technologies reported here further reduce the reflectance to below 1%, significantly improving user experience under strong ambient illumination.

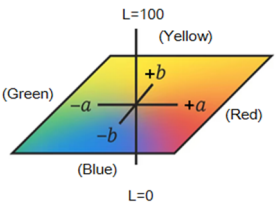

Figure 6. Schematic illustration of reflection hue.

Beyond the magnitude of reflectance itself, users are increasingly sensitive to reflection hue, which determines the integrated-black perception of the panel under off-state and dark-scene conditions. In COE structures, the reflection spectrum can be adjusted by scanning CF thickness, enabling reflection-hue optimization. This approach is compatible with multiple emission-material systems. We evaluate reflection hue using the CIE L*a*b* color space, as shown in **Figure 6**, where R% denotes the normal-incidence reflectance, a* represents the red–green axis, and b* represents the yellow–blue axis. The engineering target is not to minimize R% at all costs, but rather to maintain R% within an ultra-low-reflectance window while simultaneously placing a* and b* within an appropriate range such that the OLED panel exhibits a neutral, non-tinted dark appearance in the off state. Reflection-color coordinates around (a*, b*) ≈ (−0.5, −0.5) are perceived as particularly favorable in subjective visual evaluation.

Although the extreme low-reflectance design already yields sufficiently low reflectance, the reflection hue tends to be slightly bluish, and the integrated-black appearance is not yet optimal. This is because the original AR coating is designed with a lower reflection component in the green region and relatively higher reflection in the red and blue regions, leading to a bluish or purplish reflection hue. On this basis, we propose an AR-coating optimization concept that further suppresses the blue and red reflection components to enhance the integrated-black appearance.

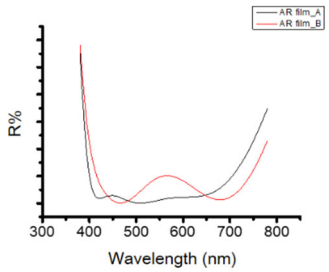

Figure 7. Schematic AR-coating reflection spectra in the visible range. Black line: conventional AR coating; red line: optimized AR coating.

Table 1. Optimized reflection-hue schemes based on different RGB CF thickness combinations

Target	Reflectance hue		
	R%	a*	b*
Ultra reflectance	0.93%	0.46	-5.98
Ultra reflectance & integrated-black	2.1%	-0.44	-0.49

We design an AR coating as shown schematically in **Figure 7** (red curve), which effectively suppresses the blue and red reflectance components while maintaining low overall reflectance. **Table 1** summarizes the detailed reflectance and reflection-hue metrics achieved by different optimization schemes developed at Visionox. It is worth emphasizing that achieving extreme low reflectance below 1% together with an enhanced integrated-black appearance inevitably requires some power-consumption trade-off. Therefore, how to alleviate power penalties and increase panel luminance under the same driving conditions, especially for outdoor usage, becomes a central focus. This aspect is discussed in detail in the next subsection.

2.2. High-Brightness and Wide-Color-Gamut Scheme

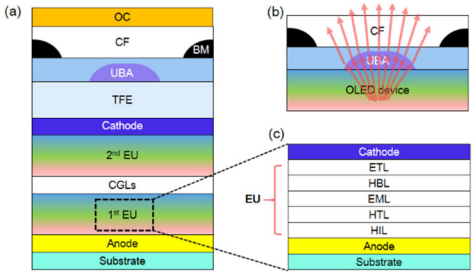

Figure 8. High-brightness optimization concept. (a) Schematic of Tandem & UBA high-brightness structure. (b) The UBA and schematic of its effect on light-extraction paths. (c) Schematic of the device emission unit structure.

One effective way to increase panel luminance is to employ tandem OLED devices. In a conventional single-stack device, there is only one emission layer; the set of layers from the hole-transport layer (HTL) to the electron-transport layer (ETL) is referred to as one emission unit (EU), as shown in **Figure 8c**. In a tandem structure, two emission units are vertically cascaded within the same pixel and are coupled via a charge-generation layer (CGL). For a given luminance, the required current density can thus be reduced, and the onset of electrical degradation is delayed [7]. In our design, each RGB subpixel adopts a tandem configuration consisting of two emission units connected in series. Introducing the tandem structure therefore brings substantial power-consumption benefits at the panel level.

On this basis, to further push the luminance ceiling, we introduce a micro-lens array (UBA) above the pixels, as depicted in **Figure 8a**. The UBA microstructures redistribute light-extraction paths and increase the fraction of near-normal emission, as illustrated schematically in **Figure 8b**. It should be noted that the UBA does not significantly alter the emission FWHM nor does it affect the microcavity length, and can therefore be regarded as an "enhanced light-extraction plugin". It boosts the luminance ceiling of the system and provides luminance margin that can be traded for reflectance reduction and enhanced integrated-black performance, thereby further improving power consumption.

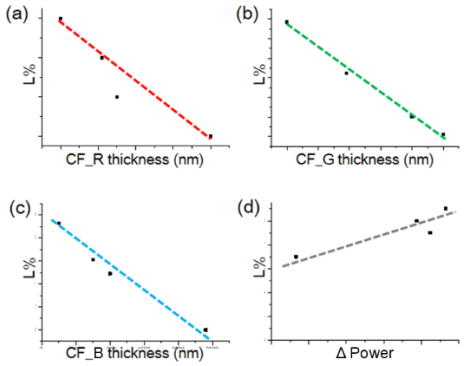

Figure 9. Trade-off between luminance and reflectance. (a)–(c) Luminance of red/green/blue subpixels as a function of CF thickness. (d) Trade-off curve between white-field power savings and panel reflectance variation.

The combination of tandem architecture and UBA enables a substantial reduction in the driving current at a given perceived luminance, resulting in considerable power savings. Meanwhile, we perform a co-optimization of the CF thickness per color channel in the COE stack, aiming to maximize panel luminance within a specified reflectance window. **Figures 9a–9c** show the functional relationships between the luminance of red, green, and blue subpixels and CF thickness. For each color, the luminance exhibits similar gain trends as the CF layer is thickened or thinned within an appropriate range. Figure 9d illustrates the overall trade-off between white-field power savings and panel reflectance variation at a given current density. There is a clear balance between luminance enhancement and low reflectance, which must be carefully optimized.

In summary, through multi-parameter co-optimization of the microcavity structure, emission materials, UBA, and CF thickness, we realize extreme high brightness, with full-screen luminance exceeding 4000 nits and panel power consumption improved by approximately 20%–40% compared with current COE products. Under the premise of maintaining low reflectance and integrated-black appearance, this provides a robust hardware foundation for further enhancing HDR display performance.

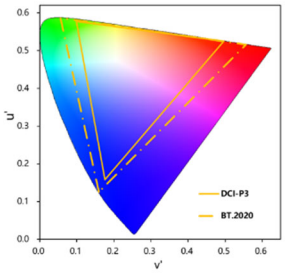

Figure 10. (a) CIE 1976 chromaticity diagram. The yellow dashed line indicates the BT.2020 standard color gamut; the yellow region indicates the DCI-P3 standard color gamut.

Color gamut is another key indicator of a display's ability to reproduce realistic colors. As industry requirements for color reproduction increase, the evaluation benchmark is shifting from DCI-P3 toward BT.2020. In this work, we use the CIE 1976 chromaticity diagram to evaluate color-gamut performance, as shown in **Figure 10**, where the yellow dashed triangle represents the BT.2020 standard gamut. The closer the vertices of a display's color-gamut triangle are to those of the BT.2020 triangle, the larger the achievable gamut coverage. In the CIE diagram, points closer to the horseshoe-shaped spectral locus correspond to higher color purity, which requires emission spectra with narrower FWHM.

However, excessively narrowing the spectrum is not always beneficial: too small an FWHM makes the device more sensitive to cavity-length variations and viewing angle, potentially introducing bottlenecks in manufacturing tolerances and viewing-angle color shift. We have compared the color-gamut coverage of POL and COE structures under different emission materials and CF designs. The results show that, by fully exploiting pTSF narrow-band emission and the optimized CF transmission spectra, the COE architecture exhibits greater potential for meeting the BT.2020 requirements.

Table 2. BT.2020 color-gamut coverage of COE panels with narrow-band emission and tandem structures

Rx	Ry	Gx	Gy	Bx	By	BT2020 @1976
0.708	0.292	0.150	0.790	0.134	0.047	98.65%

Table 2 summarizes the BT.2020 coverage levels achieved by Visionox COE panels that combine narrow emission spectra with tandem device structures. The maximum BT.2020 coverage reaches approximately 98.65%. Moreover, the BT.2020 blue vertex has a peak wavelength of about 467 nm, which is slightly red-shifted relative to conventional blue emission. This red shift is beneficial for reducing the blue-light hazard index, thereby reconciling high-brightness display performance with eye-protection requirements.

Table 3. Optical performance summary for COE-based OLED display designs

Design scheme	Key optical metrics
Extreme low-reflectance	Reflectance 0.93%; color coordinates a*, b* = 0.46, −5.98
Low-reflectance & integrated-black	Reflectance 2.1%; color coordinates a*, b* = −0.44, −0.49
High-brightness	Full-screen HBM 4100 nits
Wide color-gamut	BT.2020 coverage 98.65%

Figure 11. Demonstration of low-reflectivity and integrated-black COE display effect.

Overall, from CF and emission-material development to structural design, our work jointly optimizes panel performance in reflectance, reflection hue, luminance, and color gamut for COE products. **Table 3** summarizes the optical performance metrics achieved by different product-design schemes. **Figure 11** shows the demonstration photos of the developed low-reflectivity and integrated-black panels.

3. Conclusion

Starting from both device and optical-structure perspectives, this work systematically proposes and validates a COE design for mobile terminals that achieves low reflectance with integrated-black appearance，high brightness and wide color gamut. Building upon the low-reflectivity COE technology, we clarify four key directions for the future evolution of COE: extreme low reflectance, optimized reflection hue (integrated-black), extreme luminance, and extreme color gamut. By narrowing the CF transmission spectra, reducing the pixel aperture ratio within acceptable limits, introducing a refractive-index transition layer, and combining these with narrow-band pTSF emission materials, we obtain extreme low reflectance (below 1%), achieving an industry-leading level of anti-reflection performance. In addition, by optimizing the AR coating attached to the panel, we substantially improve the integrated-black display appearance of COE panels. On this basis, by incorporating tandem device structures and the ultra brightness array, simulations predict a 20%–40% improvement in power consumption compared with existing COE implementations, while enabling full-screen luminance above 4000 nits and BT.2020 gamut coverage of 98.65%. At the same time, the slightly red-shifted blue primary helps reduce blue-light hazard, improving visual comfort across diverse usage scenarios. Taken together, this work achieves a practically manufacturable balance among reflectance, reflection hue (integrated-black), luminance, and color gamut, and provides a scalable technology roadmap for next-generation low-reflectivity integrated-black COE OLED smartphone displays.

4. Author Biography

Dr. Ying Shen is the General Manager of the Product Engineering Center at Visionox. As a core expert in OLED technology within the company, she is primarily responsible for product engineering and technological breakthroughs in the field of OLED displays.

5. References

1. Liu X., Yu Z., Lou Z., Gao Y., Wang H., Ha M., et al. An Anode Cap Structure for Reducing Reflectance in OLED Displays. SID Symposium Digest of Technical Papers. 2025, 56: 1524-1525.
2. Li GM, Li BY, Zhang D, Liu B, Li MZ, Wang HY, et al. High efficiency and high color purity green OLEDs with narrow spectra emission. SID Symp Digest Tech Pap. 2023, 54:174–177.
3. Li GM, Zhang D, Li BY, Cai MH, Wang HY, Song WJ, et al. High performance and high color purity green OLEDs with narrow spectra emission. SID Symp Digest Tech Pap. 2024, 55: 2150–2153.
4. Cai MH, Li GM, Huang GM, Zhang YW, Zhang DD, Ha M, et al. Ultra-efficient fourth-generation pTSF OLED devices and products. SID Symp Digest Tech Pap. 2025, 56: 848–851.
5. Li GM, Li BY, Cai MH, Ha M, Song WJ, Shen Y, et al. Development of wide color-gamut green OLED devices for Adobe and BT2020 requirements. SID Symp Digest Tech Pap. 2025, 56: 656–660.
6. Swinehart D. F. The beer-lambert law. Journal of chemical education, 1962, 39: 333.
7. Han X., Han J., He M., Han C., Guo L., Yu H., et al. Achieving over 30% photon-to-photon efficiency with tandem OLED structures in organic upconversion devices. Journal of Materials Chemistry C, 2025,13: 11814-11822.